Catalysis Today 141 (2009) 264–270

Contents lists available at ScienceDirect

Catalysis Today

journal homepage: www.elsevier.com/locate/cattod

The role of Sb and Nb in rutile-type Sn/V/Nb/Sb mixed oxides, catalysts for propane ammoxidation to acrylonitrile

Nicola Ballarini [a,b], Fabrizio Cavani [a,b,*], Sergio Di Memmo [a], Francesca Zappoli [a], Philippe Marion [c]

[a] Dipartimento di Chimica Industriale e dei Materiali, Università di Bologna, Viale Risorgimento 4, 40136 Bologna, Italy
[b] INSTM, Research Unit of Bologna, A Partner of NoE Idecat, FP6 of the EU, Italy
[c] Rhodia Operations, Centre de Recherches et Technologies, 85 Rue des Frères Perret, 69190 Saint Fons, France

ARTICLE INFO

Article history:
Available online 18 October 2008

Keywords:
Propane ammoxidation
Acrylonitrile
Rutile
Tin vanadium antimony mixed oxides
Niobium oxide

ABSTRACT

This paper describes the role of Sb and Nb, components of Sn/V/Nb/Sb mixed oxides catalysts for the gas-phase ammoxidation of propane to acrylonitrile. In samples without Nb and with atomic ratios Sn/V/Sb 1/0.2/x (x = 0 to 3), Sb in the form of amorphous oxide is necessary in order to obtain an active and selective catalyst. However, during reaction the dispersed Sb oxide segregates to α-Sb_2O_4, and the yield to acrylonitrile decreases considerably. The addition of Nb gives rise to the formation of Nb-containing SbO_x and non-stoichiometric rutile-type V/Nb/Sb mixed oxides. The presence of these compounds enhances the catalytic activity and the selectivity to acrylonitrile. Moreover, the catalyst shows a stable catalytic performance, with no segregation of α-Sb_2O_4.

1. Introduction

One of the most important challenges in the modern chemical industry is the development of new processes allowing the exploitation of alternative raw materials, in replacement of technologies that make use of building blocks derived from oil (olefins and aromatics). This has led to research for the valorization of natural gas components, through catalytic processes of transformation [1,2]. One reaction investigated since many years is the direct ammoxidation of propane to acrylonitrile [3–5]. Different types of catalytic systems have been described in the literature for this reaction: (a) multicomponent rutile-type V-antimonates (e.g., V/Sb/W/Al/O) [3,4], (b) monophasic multicomponent molybdates (Mo/V/Nb/Te(Sb)/O) [6], (c) V/Al mixed oxynitrides [7,8], and Al/Ga/P/O-supported vanadium oxide [9,10]. Multimetal molybdates, developed by Mitsubishi Kasei, give the highest yield to acrylonitrile under propane-lean conditions. Rutile-type mixed oxides may contain several elements aimed at different roles in the complex transformation of the alkane [11–13]. In regard to this, the rutile structure possesses the flexibility required to accommodate various elements in its framework.

In previous works [14,15] we described a method for the preparation of rutile-type Sn/V/Sb mixed oxides that includes the co-precipitation of the metal oxo-hydrates from an alcoholic solution. The thermal treatment of the precipitate leads to the development of nano-sized rutile crystalites, that compared to the more crystalline rutile systems prepared with the conventional "slurry" method are characterized by a greater structural defectivity, a higher specific surface area and hence a higher catalytic activity in propane ammoxidation.

In the present work, we report on the role of Sb and on the effect of Nb addition in Sn/V/Nb/Sb/O catalysts. Niobium is known to be an important component in catalysts for the selective oxidation of hydrocarbons [16,17], and also enhances the selectivity to acrylonitrile from propane in Cr/V/Sb/O [18] and V/Sb/O catalysts [19,20].

2. Experimental

Catalysts were prepared with the co-precipitation technique, developed for the synthesis of rutile SnO_2-based systems claimed by Rhodia [14]. The preparation involves the dissolution of $SnCl_4{\cdot}5H_2O$, $VO(acac)_2$, $SbCl_5$ and $NbCl_5$ in absolute ethanol; the alcoholic solution is then dropped into a buffered aqueous solution maintained at pH 7. The precipitate obtained is separated from the supernatant liquid by filtration. The solid is then dried at 120 °C, and calcined in air at 700 °C for 3 h.

The X-ray diffraction patterns of the catalysts were obtained with Ni-filtered Cu Kα radiation on a Philips X'Pert vertical diffractometer equipped with a pulse height analyzer and a secondary curved graphite-crystal monochromator. The crystal size of rutile samples

* Corresponding author at: Dipartimento di Chimica Industriale e dei Materiali, Università di Bologna, Viale Risorgimento 4, 40136 Bologna, Italy.
E-mail address: fabrizio.cavani@unibo.it (F. Cavani).

0920-5861/$ – see front matter © 2008 Elsevier B.V. All rights reserved.
doi:10.1016/j.cattod.2008.08.041

was measured by applying the Sherrer equation to the three most intense reflections in the XRD pattern.

Laser-Raman spectra were obtained using a Renishaw 1000 instrument; the samples were excited with the 514 nm Ar line. Spectra were recorded at room temperature. Specific surface areas were measured by the single-point, BET method with nitrogen adsorption (Thermo Instrument).

Catalytic tests were carried out in a laboratory glass fixed-bed tubular reactor operating at atmospheric pressure. 1.8 g of catalyst was loaded, shaped into particles with size ranging from 0.42 to 0.55 mm. The following reaction conditions were used: feed composition 25 mol.% propane, 10% ammonia, 20% oxygen, remainder helium; residence time 2.0 s. The reactor outlet was kept at 170 °C. On-line sampling of a volume of either the feedstock or effluents was obtained by means of three heated valves. Three different columns were used for the product identification. Two of these were: a Hay-sep T column (TCD detector) for the separation of CO_2, NH_3, $C_3H_8 + C_3H_6$, H_2O, HCN, acrolein, acetonitrile and acrylonitrile, and a MS-5A column (TCD detector) for separation of O_2, N_2 and CO. Hay-sep T was also used as a filter to avoid the contamination of MS-5A by CO_2. The third column was a packed column filled with Poropak QS (FID detector), which is used for the separation of propane from propylene. Selectivity and yield to each reaction product were calculated considering the reaction stoichiometry. Temperature gradients in the catalytic bed along the axial direction were measured; the maximum temperature difference was 8 °C. The temperatures reported in Figures were those recorded in correspondence of the hot spot in the catalytic bed.

Catalytic measurements were taken after approximately 10 h reaction time (equilibration period); with all catalysts, the performance was stable after this initial period. In most cases, there were negligible deactivation phenomena during equilibration; with some catalysts, however, deactivation phenomena were evident (see Section 3.4).

3. Results and discussion

3.1. Characterization of calcined Sn/V/Nb/Sb 1/0.2/0/x catalysts

Table 1 reports the theoretical atomic composition of samples, calculated on the basis of the amount of each precursor used for the preparation, the corresponding experimental composition for a few of them (as determined by X-ray fluorescence) and the values of specific surface area. Two series of samples were prepared with composition Sn/V/Nb/Sb 1/0.2/0/x ($0 \le x \le 3$, atomic ratios between components) and Sn/V/Nb/Sb 1/0.2/y/3 ($0 \le y \le 3$). The XRF analysis was in good agreement with the theoretical compositions; this was true for both samples having low and high Sb content. Therefore, theoretical compositions were assumed to correspond to the real ones for all samples prepared. The atomic ratio between Sn and V was fixed at 1/0.2 because this ratio was found to be the optimal one in Sn/V/Sb mixed oxides [14].

Table 1
Theoretical and experimental (X-ray fluorescence) bulk atomic composition, and specific surface area of catalysts prepared

Atomic composition (theoretical)	Atomic composition (experimental)	Specific surface area (m^2/g)
Sn/V/Nb/Sb 1/0.2/0/0	1.00/0.19/0/0	40
Sn/V/Nb/Sb 1/0.2/0/1	1.00/0.20/0/0.95	55
Sn/V/Nb/Sb 1/0.2/0/2	nd	63
Sn/V/Nb/Sb 1/0.2/0/3	nd	35
Sn/V/Nb/Sb 1/0.2/1/3	1.00/0.20/1.16/2.81	74
Sn/V/Nb/Sb 1/0.2/3/3	nd	33

nd: not determined.

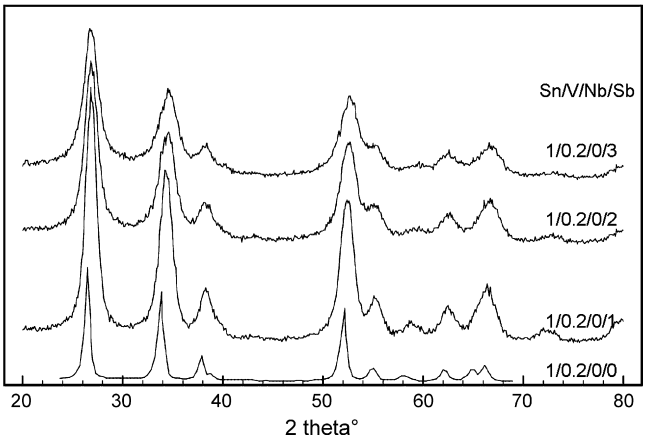

Fig. 1. XRD patterns of calcined Sn/V/Nb/Sb 1/0.2/0/x samples.

The surface area of samples was remarkably higher than that one typically reported for rutile-type mixed oxides prepared with conventional methodologies like the slurry-redox, leading to surface areas systematically lower than 10 m^2/g. There was no significant effect of the composition on the surface area; for all samples, the latter was higher than 40 m^2/g, with the exception of the sample without Nb and containing the greater amount of Sb (Sn/V/Nb/Sb 1/0.2/0/3, 35 m^2/g), and of the sample containing the greater amounts of both Sb and Nb (Sn/V/Nb/Sb 1/0.2/3/3, 33 m^2/g).

Catalysts based on Sn/V/O prepared by co-precipitation were studied in previous works [21,22]. It was found that the solubility of V^{4+} in cassiterite is low; the maximum value of z in the $Sn_{1-z}V_zO_2$ substitutional solid solution was approximately 0.10. The rest of vanadium was dispersed in the form of polymeric species over tin oxide [21–23]. The XRD patterns showed the reflections of cassiterite, with a slight contraction of the crystallographic parameters for the tetragonal cell with respect to SnO_2 ($z = 0$), because of the incorporation of V^{4+} [21]. The crystal size of sample Sn/V/Nb/Sb 1/0.2/0/0 calcined at 700 °C was 17 ± 3 nm. In samples prepared with an atomic Sn/V ratio lower than 1/0.2, also crystalline V_2O_5 formed [21,22].

The X-ray diffraction patterns of samples Sn/V/Nb/Sb 1/0.2/0/x are reported in Fig. 1. All patterns show the reflections typical of rutile SnO_2 cassiterite (JCPDS 005-0467). The addition of Sb led to a decrease of the crystallinity of samples; the crystal size of samples having $x > 0$ was 8 ± 2 nm. This can be attributed to the dissolution of Sb^{5+} in the cassiterite lattice [24,25], and to the generation of cationic vacancies.

Before discussing the Raman spectra of samples Sn/V/Nb/Sb 1/0.2/0/x (reported in Fig. 2), it is worth reminding the typical Raman features of reference single and binary oxides. Tin oxide, when prepared with the same precipitation procedure adopted for multicomponent samples, has a strong Raman band at 625–630 cm^{-1} and weaker ones at 770 and 685 cm^{-1}, all corresponding to bulk vibration modes [26,27]. A band is at 555 cm^{-1} (surface mode), the relative intensity of which is a function of the sample surface area, and hence of the temperature of thermal treatment. The Raman spectrum of hydrated Nb oxide, when calcined at temperatures between 500 and 700 °C, shows a broad band at 680–690 cm^{-1} and less intense bands at 140, 220 and 310 cm^{-1}. The thermal treatment of Nb oxide at temperatures higher than 700 °C yields to a completely different spectrum, with a strong band at 1000 cm^{-1}, assigned to terminal niobyl species, two intense bands between 700 and 800 cm^{-1} and one below 300 cm^{-1} [28–30]. After calcination at 1000 °C, the monoclinic form of niobium oxide

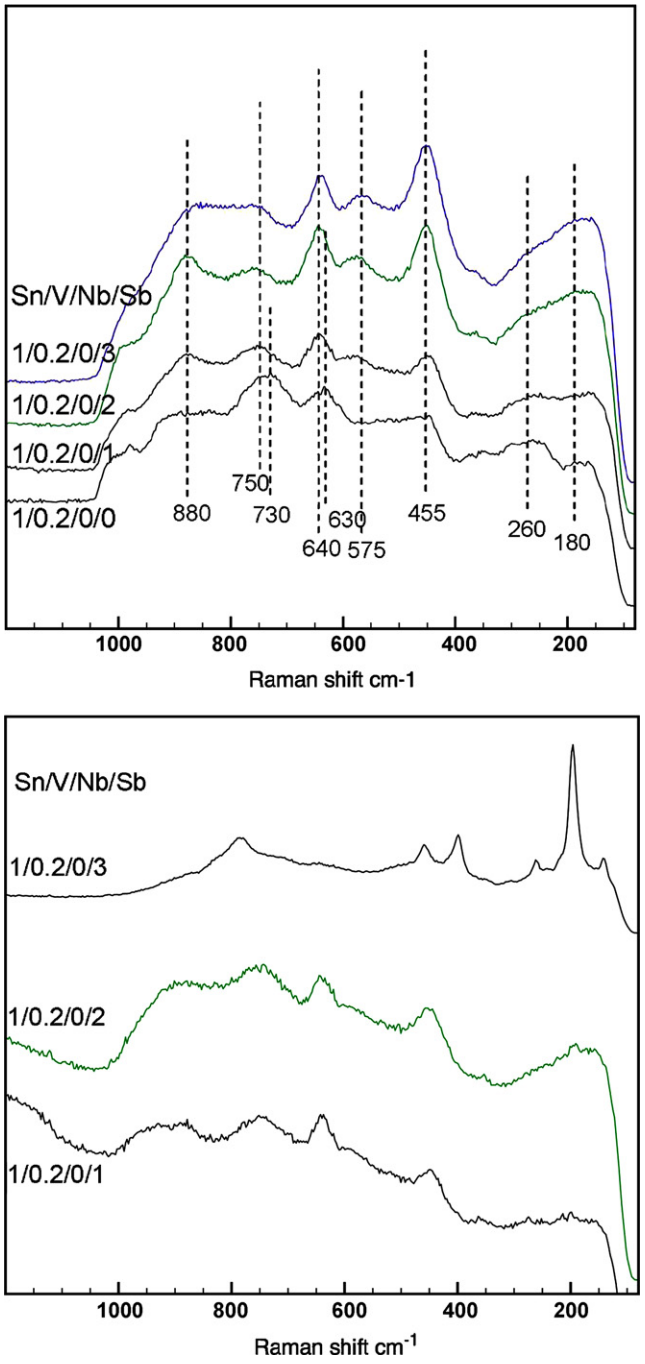

Fig. 2. Top: Raman spectra of calcined Sn/V/Nb/Sb 1/0.2/0/x samples. Bottom: Raman spectra of used Sn/V/Nb/Sb 1/0.2/0/x samples.

(H–Nb_2O_5) shows bands at 992, 674, 623, 261 and 236 cm^{-1}. The Raman spectrum of rutile $VNbO_4$ has bands at 990, 920 and 620 cm^{-1} [31,32]; however, this compound is stable at temperatures higher than 500 °C only under O_2-free atmosphere. Nb-rich V/Nb mixed oxides, e.g., VNb_9O_{25} or $V_4Nb_{18}O_{55}$, are obtained by thermal decomposition in air at 700 °C of orthorhombic $VNbO_5$ [31,32]. The spectrum of $SbNbO_4$ exhibits bands at 845, 685, 620 and 380 cm^{-1} [19,20], whereas the spectrum of quasi-$VSbO_4$ has very broad features [11].

The Raman spectrum of sample Sn/V/Nb/Sb 1/0.2/0/0 (Fig. 2) shows marked differences with respect to that of SnO_2. In literature, a broad band between 900 and 1000 cm^{-1} in dehydrated Sn/V/O samples is assigned to the ν (V=O) stretching mode of the polymeric VO_x [27], while a band at 840 cm^{-1} is assigned to the specific V–O–Sn stretching mode in an interfacial region, and an intense band at 480 cm^{-1} to polymeric species. In our Sn/V/O sample, all bands are attributable either to the polymeric vanadia species, or to the bulk modes of tin oxide. The intense broad band between 720 and 750 cm^{-1} is attributable to the polymeric species in hydrated supported vanadium oxide catalysts [33,34].

The addition of Sb (Sn/V/Nb/Sb 1/0.2/0/x with x = 1–3) caused the formation of new features in the Raman spectrum. In fact, new bands appeared at 180–200 and 455 cm^{-1}, attributable to β-Sb_2O_4 and Sb_6O_{13}, respectively. However, the 100% intensity band of Sb_6O_{13} should fall at 470 cm^{-1}; the relevant shift observed with our samples (455 vs. 470 cm^{-1}) might be due to the dissolution of Sn^{4+} ions inside the Sb oxide lattice. Also the shift from 630 to 640 cm^{-1} of the band assigned to SnO_2 can be attributed to the formation of a Sn/Sb mixed oxide. In fact, the Raman spectrum of a reference Sn/Sb/O sample, prepared by calcination of an Sn/Sb 1/1 precipitate, had two strong Raman bands at 640 and 455 cm^{-1}. The decrease of intensity of the bands attributed to the dispersed vanadium oxide indicates that vanadium likely formed a rutile-type V/Sb/O.

3.2. Catalytic performance of Sn/V/Nb/Sb 1/0.2/0/x catalysts

The catalytic performance of samples Sn/V/Nb/Sb 1/0.2/0/x is summarized in Fig. 3, showing the conversion of propane and oxygen, and the selectivity to acrylonitrile as functions of the reaction temperature. The distribution of products is also reported, obtained in correspondence with the highest acrylonitrile yield.

The sample with composition Sn/V/Nb/Sb 1/0.2/0/0 (not reported) was very active, but gave exclusively propylene and carbon oxides. The progressive increase of the Sb content led to a decrease of catalytic activity; the catalyst with x = 1 gave 21% propane conversion and 100% oxygen conversion at 440 °C, while the catalyst with x = 3 reached the same conversion at 525 °C.

In the case of the catalyst with x = 1, the maximum selectivity to acrylonitrile was obtained at total oxygen conversion, whereas with the catalyst having x = 2, the selectivity to acrylonitrile declined slightly when the conversion of oxygen reached the 100%. The fall of selectivity was dramatic when the temperature was increased from 490 to 525 °C with the catalyst having x = 3. At the latter temperature, i.e., at conditions of 100% oxygen conversion, the catalyst underwent irreversible changes. In fact, when the performance was tested again at 490 °C, the selectivity to acrylonitrile measured was lower than that one formerly obtained at the same temperature (15% vs. 45%), whereas the conversion of propane was the same (20%). Interestingly, the variation of selectivity was negligible when the maximum reaction temperature was kept lower than that one at which oxygen conversion was total.

On the opposite, the catalyst with x = 1 showed a stable catalytic performance, even when the reaction was carried out at conditions of total oxygen conversion. On the other hand, Fig. 3 (bottom) shows that the greater was the amount of Sb in the catalyst, the higher was the maximum selectivity to acrylonitrile, and the lower the formation of CO_x and HCN. In literature, it is reported that in order to be selective in propane ammoxidation, a V/Sb/O catalyst should have amorphous antimony oxide dispersed over the rutile $VSbO_4$ [4]. In fact, antimony oxide contains the Sb–O–Sb sites that in the presence of gas-phase ammonia are converted into Sb–NH–Sb species [4]. These sites perform the $(NH)^{2-}$ insertion onto the allylic intermediate.

3.3. The reaction network in propane ammoxidation

The catalytic performance of sample Sn/V/Nb/Sb 1/0.2/0/2 is shown in Fig. 4 as a function of the reaction temperature. At low

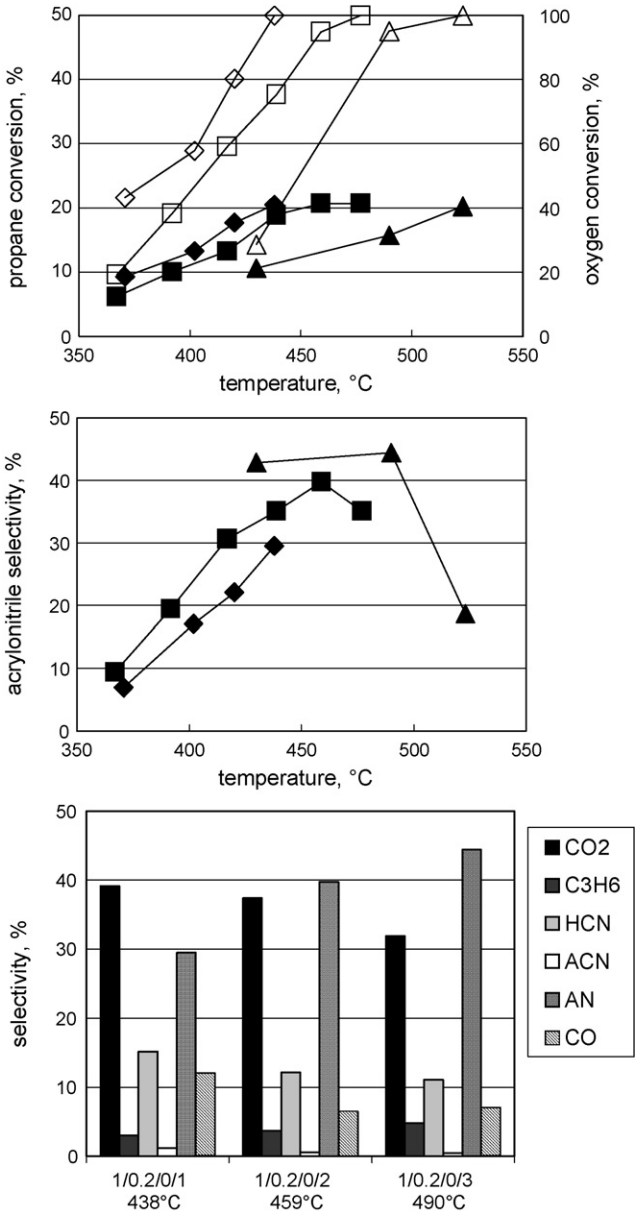

Fig. 3. Catalytic performance of Sn/V/Nb/Sb 1/0.2/0/*x* samples. Top: propane conversion (full symbols) and oxygen conversion (open symbols) as functions of temperature. Middle: selectivity to acrylonitrile as a function of temperature. Symbols: Sn/V/Nb/Sb 1/0.2/0/1 (◆◇), 1/0.2/0/2 (■□) and 1/0.2/0/3 (▲△). Bottom: selectivity to each product at the temperature of maximum acrylonitrile yield (CO_2: carbon dioxide; C_3H_6: propylene; HCN: cyanhydric acid; ACN: acetonitrile; AN: acrylonitrile; CO: carbon monoxide).

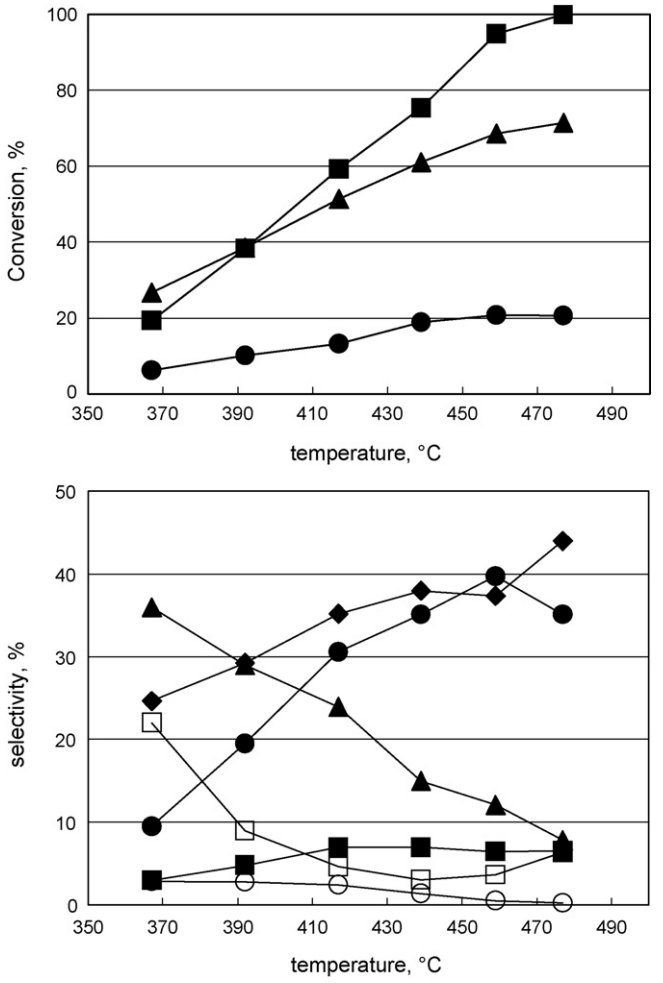

Fig. 4. Effect of temperature on catalytic performance of Sn/V/Nb/Sb 1/0.2/0/2 sample. Top: conversion of propane (●), ammonia (▲) and oxygen (■). Bottom: selectivity to acrylonitrile (●), acetonitrile (○), carbon dioxide (◆), carbon monoxide (■), propylene (□) and cyanhydric acid (▲). Residence time 2 s.

temperature, the main reaction products were cyanhydric acid, propylene and carbon dioxide. The selectivity to acrylonitrile at 355 °C was less than 10%; CO and acetonitrile formed with selectivity lower than 5%.

The increase of temperature led to a decrease of the selectivity to propylene and to cyanhydric acid, and to the concomitant increase of the selectivity to acrylonitrile; the latter reached a maximum value at 460 °C. These data suggest that the catalyst transforms propane into propylene by oxidative dehydrogenation; then, the olefin is converted into the allylic intermediate by $H^{\bullet}$ abstraction. At low temperature, however, the latter is preferentially transformed into lighter radical fragments, which either yield CO_2 or react with activated ammonia to generate HCN. When the temperature is increased, the ammoxidation to acrylonitrile becomes the preferred pathway of transformation of the allylic intermediate, and the selectivity to HCN decreases. It is possible that the key factor for the control of the two competing reactions is the generation of the active species Me = NH, favoured at high temperature. At low temperature, the low concentration of these sites makes the desorption of propylene or its cracking into lighter compounds become the preferred reaction pathway.

Fig. 5 shows the effect of the residence time on the conversion of reactants and the distribution of products, at 440 °C, i.e., at conditions that are kinetically more favourable for the formation of acrylonitrile and less for cyanhydric acid. The data clearly indicate that the primary reaction products are propylene, CO_2, CO and acetonitrile. Acrylonitrile and cyanhydric acid are both secondary products, formed by transformation of propylene. Moreover, CO and CO_2 are also formed by consecutive reactions occurring on propylene. For residence time higher than 0.5–1.0 s, a consecutive reaction to CO_2 is responsible for the decline of the selectivity to acrylonitrile.

Fig. 6 summarizes the reaction scheme at 440 °C; the network is similar to that one found for rutile-type Cr/V/Sb/O catalysts [35].

These data confirm that the main reactions leading to the CN-containing compounds start from the intermediate olefin. The relative contribution of the two parallel reactions leading either to

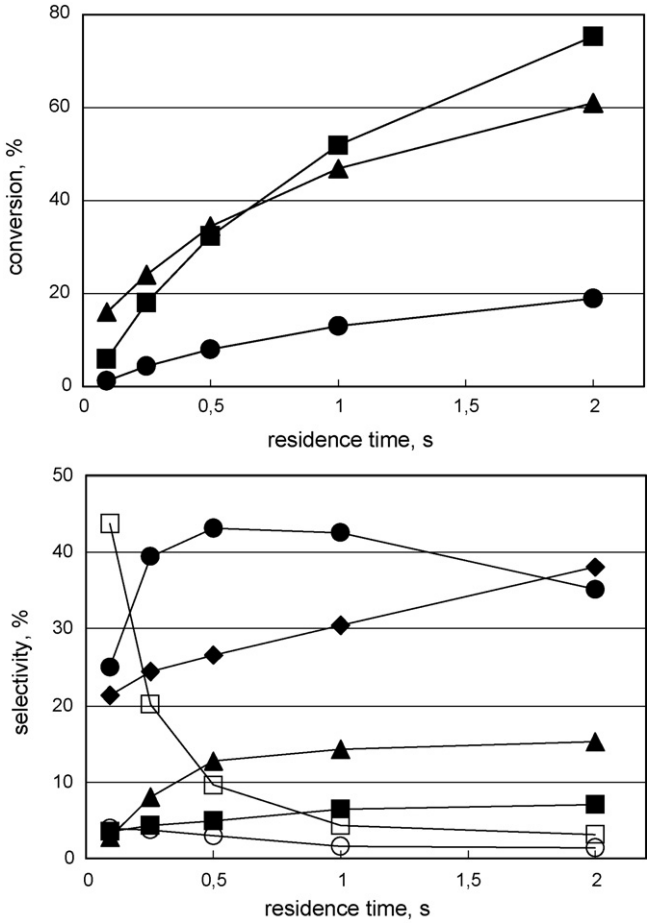

Fig. 5. Effect of residence time on catalytic performance of Sn/V/Nb/Sb 1/0.2/0/2 sample. Top: conversion of propane (●), ammonia (▲) and oxygen (■). Bottom: selectivity to acrylonitrile (●), acetonitrile (○), carbon dioxide (◆), carbon monoxide (■), propylene (□) and cyanhydric acid (▲). Temperature 440 °C.

acrylonitrile or to HCN + CO_x, is a function of the reaction temperature. Therefore, the key-factor for the control of the selectivity to acrylonitrile is the availability of surface allylic ammoxidation sites, the latter being a function of the temperature and of the amount of Sb oxide in catalysts. In general, higher temperatures and higher amounts of Sb oxide are parameters in favour of the selectivity to acrylonitrile. The most selective Sn/V/Sb 1/0.2/*x* catalyst is that one having *x* = 3, and Sb oxide dispersed over the rutile; however, this catalyst is unstable under reaction conditions that lead to total oxygen conversion (Fig. 3).

3.4. Characterization of used Sn/V/Nb/Sb 1/0.2/0/x catalysts

Fig. 2 (bottom) reports the Raman spectra of Sn/V/Nb/Sb 1/0.2/0/*x* catalysts after reactivity tests. Raman spectra of used samples

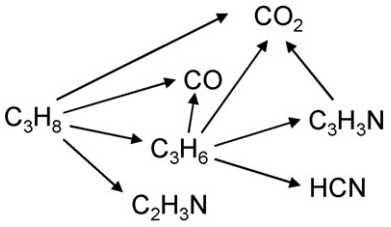

Fig. 6. Reaction scheme for propane ammoxidation at 440 °C. Co-reactants (NH_3 and O_2) and co-products (H_2O, N_2) have been omitted.

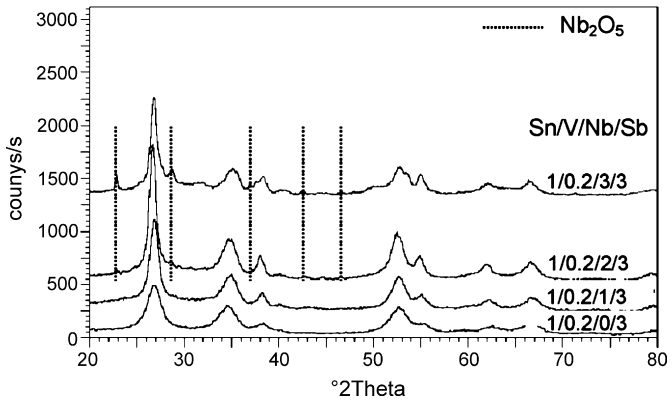

Fig. 7. XRD patterns of calcined Sn/V/Nb/Sb 1/0.2/*y*/3 samples.

with *x* = 1 and 2 were very similar to the spectra of corresponding fresh samples (Fig. 2 top). On the contrary, the spectrum of the used catalyst with *x* = 3 was different from that one of the fresh sample. In fact, new Raman bands were present, attributable to vibrations of α-Sb_2O_4. Therefore, the fall of selectivity to acrylonitrile shown at high temperature (Fig. 3) was due to the transformation of dispersed Sb oxide into α-Sb_2O_4.

These data indicate that in order to obtain a catalyst offering the best performance, it is necessary to stabilize the amorphous Sb oxide phase, the key-component for the selectivity to acrylonitrile.

3.5. Characterization of calcined Sn/V/Nb/Sb 1/0.2/y/3 catalysts

Samples were prepared by keeping the Sn/V/Sb atomic ratio fixed (1/0.2/3), and by adding increasing amounts of Nb. Nb was chosen as a promoter, because of its positive effect on selectivity observed with the rutile-type Cr/V/Sb/O catalysts [18].

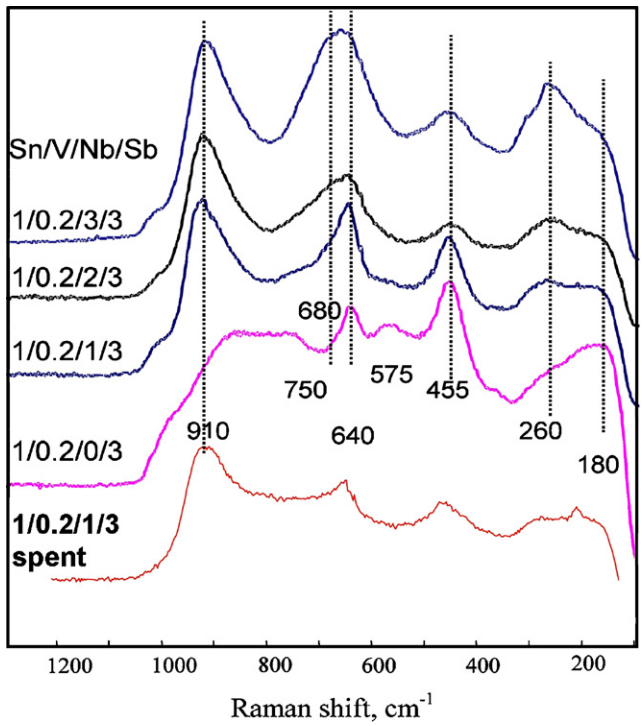

Fig. 8. Raman spectra of calcined Sn/V/Nb/Sb 1/0.2/*y*/3 and used Sn/V/Nb/Sb 1/0.2/1/3 samples.

X-ray diffraction patterns and Raman spectra of samples with composition Sn/V/Nb/Sb 1/0.2/y/3 are reported in Figs. 7 and 8, respectively. The XRD pattern for these samples corresponds to that one of the rutile structure; additional lines observed for the sample with the higher Nb content (y = 3) are attributed to orthorhombic Nb_2O_5 (JCPDS 27-1013).

For what concerns the Raman spectra, the presence of Nb led to the decrease of the intensity of the band at 455 cm^{-1}, attributed to the Sn-doped Sb oxide; this suggests the preferential formation of a Nb/Sb oxide. An analogous behavior was observed in the case of Cr/V/Nb/Sb/O systems [18], in which the development of a mixed vanadium antimonate/niobate was the reason for the presence of lower amounts of dispersed Sb oxide than in Cr/V/Sb/O catalysts.

A peculiar property of rutile-type oxides is the ability of hosting large concentration of cationic vacancies, and developing defective structures. This occurs, for instance, in rutile-type mixed oxides such as quasi-$VSbO_4$, Fe/V/Sb, Cr/V/Sb and Mo/V/Sb mixed oxides [11,12,18,36], in which vacancies are formed because of either the excess positive charges generated by oxidation of V^{3+}–V^{4+} and V^{5+}, or the incorporation of altervalent cations in rutile lattice. The development of a band at 920 cm^{-1} (Fig. 8) in samples containing Nb suggests the formation of cationic vacancies in Sn/V/Nb/Sb/O samples. Vacancies may develop by formation of a mixed V antimonate/niobate and replacement of either Sb^{3+} or V^{3+}/V^{4+} for Nb^{5+} [37].

In samples having the higher Nb content (y = 2 and 3), bands at 670–680 and 250–260 cm^{-1} can be attributed to orthorhombic Nb_2O_5 [28–30].

3.6. Catalytic performance of Sn/V/Nb/Sb 1/0.2/y/3 catalysts

Fig. 9 reports the results of catalytic tests with Sn/V/Nb/Sb 1/0.2/y/3 samples. The activity of catalysts with y = 0 and y = 1 was similar; both samples gave total conversion of oxygen at 520–530 °C (Fig. 9 top). However, in the former case the selectivity to acrylonitrile decreased considerably when the temperature was increased from 490 to 525 °C; in the case of the catalyst with y = 1, the decline of selectivity was less evident. Catalysts having the higher amount of Nb (y = 2 and 3) were even more active; both gave total oxygen conversion at 480–490 °C. However, the selectivity to acrylonitrile at total oxygen conversion was lower than that obtained with the catalyst having y = 1.

Fig. 9 (bottom) shows the distribution of products, obtained at the temperature of the highest acrylonitrile yield. The addition of Nb led to an increase of the selectivity to CO, propylene and acetonitrile, and to a relevant decrease of the selectivity to CO_2, but it did not affect the formation of HCN. The selectivity to acrylonitrile reached a maximum in correspondence with the intermediate Nb content (y = 1). Therefore, as long as Nb was present in a relatively low amount, it improved the selectivity of sites responsible for the allylic ammoxidation of propylene. At higher Nb content, crystalline Nb_2O_5 formed and this led to a further slight decline of the selectivity to CO_2, but also to a higher formation of CO and to a lower efficiency in allylic ammoxidation.

The maximum yield to acrylonitrile achieved with the Sn/V/Nb/Sb 1/0.2/1/3 catalyst, 11%, falls in the range typically obtained with rutile-type catalysts under hydrocarbon-rich conditions, but is lower than the yield obtained under propane-lean conditions with the Mo/V/Nb/Te/O system [6].

The Raman spectrum of the used Sn/V/Nb/Sb 1/0.2/1/3 catalyst is shown in Fig. 8; the comparison with the spectrum of the fresh sample confirms that in this case the segregation of α-Sb_2O_4 during reaction was minimal. Therefore, the incorporation of Nb^{5+} in the dispersed Sb oxide improved the structural stability and the efficiency in allylic ammoxidation of the latter compound.

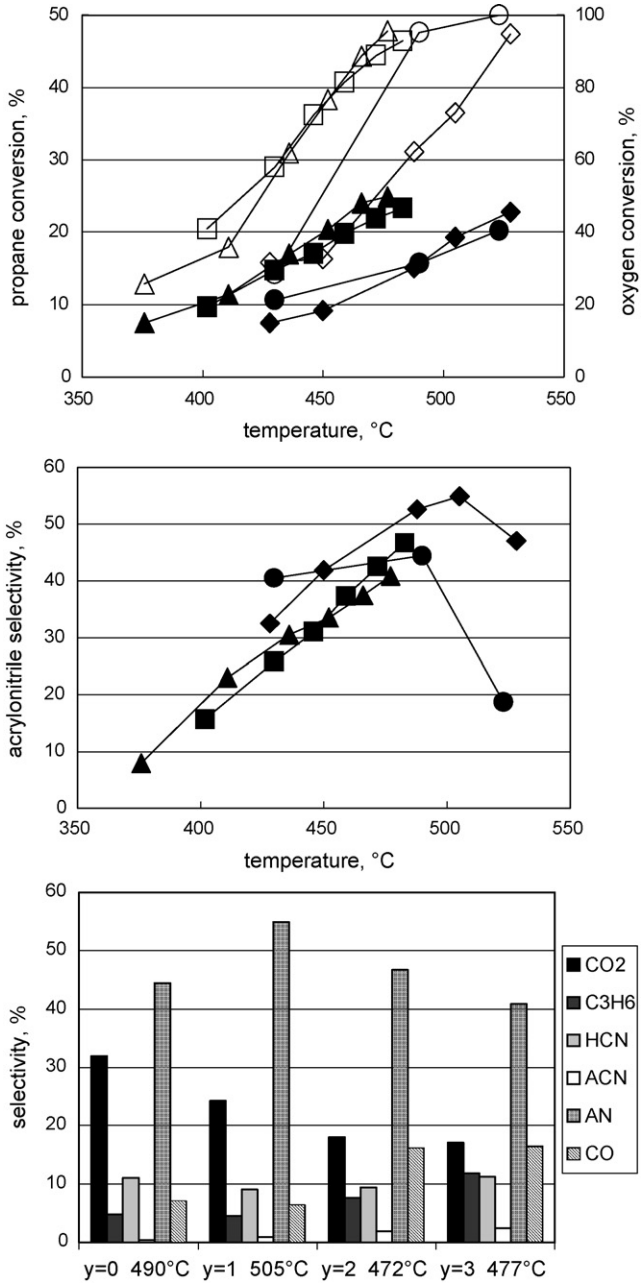

Fig. 9. Catalytic performance of Sn/V/Nb/Sb 1/0.2/y/3 samples. Top: propane conversion (full symbols) and oxygen conversion (open symbols) as functions of temperature. Middle: selectivity to acrylonitrile as a function of temperature. Symbols: Sn/V/Nb/Sb 1/0.2/0/3 (●○), 1/0.2/1/3 (◆◇), 1/0.2/2/3 (■□) and 1/0.2/3/3 (▲△). Bottom: selectivity to each product at the temperature of maximum acrylonitrile yield (CO_2: carbon dioxide; C_3H_6: propylene; HCN: cyanhydric acid; ACN: acetonitrile; AN: acrylonitrile; CO: carbon monoxide).

The characterization by Raman spectroscopy indicates that Nb is not only incorporated in to the Sb oxide, but also generates a defective, rutile-type V/Nb/Sb mixed oxide. The Nb content affects the concentration of vacancies in the latter compound. It is known that vacancies may affect the H-abstracting properties of V^{4+} in rutile and the N-insertion properties of Me = NH sites [11,12,18,36,38]. Therefore, in our catalysts an increasing concentration of vacancies may be the reason for the enhancement of catalytic activity.

The stability of the Sn/V/Nb/Sb 1/0.2/1/3 catalyst was also confirmed by medium-term lifetime measurements carried out over 25 h reaction time. The morphological features were also

maintained, i.e., the nano-size of rutile crystalites remained unchanged during catalytic measurements.

4. Conclusions

Sn/V/Sb mixed oxides are efficient catalysts for the ammoxidation of propane to acrylonitrile under hydrocarbon-rich conditions. The catalysts, when prepared by co-precipitation from an alcoholic medium and calcined at 700 °C, consist of nano-sized crystals with surface area higher than 40 m^2/g. Tin dioxide incorporates Sb cations, and provides the rutile matrix for the dispersion of the active components. In these catalysts, an excess Sb is necessary in order to form an amorphous Sb oxide (probably also containing Sn^{4+}), that is highly efficient in the allylic ammoxidation of the intermediately formed propylene. However, the most selective catalyst is also the least stable, since the amorphous Sb oxide segregates into the inactive α-Sb_2O_4 when reaction conditions are used that lead to the total conversion of the limiting reactant, oxygen. With rutile-based catalysts, the latter are the conditions of maximum acrylonitrile yield under propane-rich conditions.

The addition of Nb^{5+} to the Sn/V/Sb/O system gives a remarkable improvement of catalytic performance and of catalyst stability. The best yield to acrylonitrile is obtained with the catalyst having composition Sn/V/Nb/Sb 1/0.2/1/3. This catalyst gives the highest selectivity to acrylonitrile under conditions of total oxygen conversion.

The incorporation of Nb^{5+} into the Sb oxide considerably improves the selectivity to acrylonitrile and the structural stability of the catalyst under reaction conditions, limiting the generation of the unselective α-Sb_2O_4. Moreover, the development of cationic vacancies in the rutile V/Sb/Nb mixed oxide is proposed to be the reason for the better activity of Nb-containing catalysts.

Acknowledgement

Rhodia is acknowledged for financial support.

References

[1] P. Arpentinier, F. Cavani, F. Trifirò, The Technology of Catalytic Oxidations, Editions Technip, Paris, 2001.
[2] F. Cavani, F. Trifirò, Basic principles in applied catalysis, in: M. Baerns (Ed.), Series in Chemical Physics, vol. 75, Springer, Berlin, 2003, p. 21.
[3] R.K. Grasselli, Top. Catal. 21 (2002) 79.
[4] G. Centi, S. Perathoner, F. Trifirò, Appl. Catal. A 157 (1997) 143.
[5] Y. Moro-oka, W. Ueda, Catalysis, vol. 11, Royal Society of Chemistry, 1994, p. 223.
[6] T. Ushikubo, K. Oshima, A. Kayou, M. Vaarkamp, M. Hatano, J. Catal. 169 (1997) 394.
[7] M. Florea, R. Prada Silvy, P. Grange, Appl. Catal. A 286 (2005) 1.
[8] M. Olea, M. Florea, I. Sack, R. Prada Silvy, E.M. Gaigneaux, G.B. Marin, P. Grange, J. Catal. 232 (2005) 152.
[9] M.A. Soria, P. Ruiz, E.M. Gaigneaux, Catal. Today 128 (2007) 168.
[10] M.A. Soria, S. Delsarte, E.M. Gaigneaux, P. Ruiz, Appl. Catal. A 325 (2007) 296.
[11] J. Nilsson, A.R. Landa-Canovas, S. Hansen, A. Andersson, J. Catal. 186 (1999) 442.
[12] H. Roussel, B. Mehlomakulu, F. Belhadj, E. Van Steen, J.M.M. Millet, J. Catal. 205 (2002) 97.
[13] V.D. Sokolovskii, A.A. Davydov, O.Yu. Ovsitser, Catal. Rev. Sci. Eng. 37 (3) (1995) 425.
[14] S. Albonetti, G. Blanchard, P. Burattin, F. Cavani, F. Trifirò, US 6,083,869, assigned to Rhodia.
[15] S. Albonetti, G. Blanchard, P. Burattin, F. Cavani, S. Masetti, F. Trifirò, Catal. Today 42 (1998) 283.
[16] M. Ziolek, Catal. Today 78 (2003) 47.
[17] I. Nowak, M. Ziolek, Chem. Rev. 99 (1999) 3603.
[18] N. Ballarini, F. Cavani, M. Cimini, F. Trifirò, J.M.M. Millet, U. Cornaro, R. Catani, J. Catal. 241 (2006) 255.
[19] M.O. Guerrero-Perez, J.L.G. Fierro, M.A. Bañares, Catal. Today 78 (2003) 387.
[20] M.O. Guerrero-Perez, J.L.G. Fierro, M.A. Bañares, Phys. Chem. Chem. Phys. 5 (2003) 4032.
[21] S. Bordoni, F. Castellani, F. Cavani, F. Trifirò, M. Gazzano, J. Chem. Soc., Faraday Trans. 2981 (90) (1994).
[22] S. Bordoni, F. Castellani, F. Cavani, F. Trifirò, M.P. Kulkarni, Stud. Surf. Sci. Catal. 82 (1994) 93.
[23] Y. Fu, H. Ma, Z. Wang, W. Zhu, T. Wu, G. Wang, J. Mol. Catal. A 221 (2004) 163.
[24] F.J. Berry, Adv. Catal. 30 (1981) 97.
[25] M. Caldararu, M.F. Thomas, J. Bland, D. Spranceana, Appl. Catal. A 209 (2001) 383.
[26] J.M. Herrmann, F. Villain, L.G. Appel, Appl. Catal. A 240 (2003) 177.
[27] S. Loridant, J. Phys. Chem. B 106 (2002) 13273.
[28] J.-M. Jehng, I.E. Wachs, Chem. Mater. 3 (1991) 100.
[29] R. Brayner, F.B. Verduraz, Phys. Chem. Chem. Phys. 5 (2003) 1457.
[30] B.X. Huang, K. Wang, J.S. Church, Y.S. Li, Electrochim. Acta 44 (1999) 2571.
[31] N. Ballarini, F. Cavani, C. Cortelli, C. Giunchi, P. Nobili, F. Trifirò, R. Catani, U. Cornaro, Catal. Today 78 (2003) 353.
[32] N. Ballarini, G. Calestani, R. Catani, F. Cavani, U. Cornaro, C. Cortelli, M. Ferrari, Stud. Surf. Sci. Catal. 155 (2005) 81.
[33] I.E. Wachs, Catal. Today 27 (1996) 437.
[34] G.G. Cortez, M.A. Banares, J. Catal. 209 (2002) 197.
[35] N. Ballarini, F. Cavani, M. Cimini, F. Trifirò, R. Catani, U. Cornaro, D. Ghisletti, Appl. Catal. A 251 (2003) 49.
[36] M. Cimini, J.M.M. Millet, F. Cavani, J. Solid State Chem. 177 (2004) 1045.
[37] Y. Mimura, K. Ohyachi, I. Matsuura, Science and Technology in Catalysis 1998, Kodansha, Tokyo, 1999, p. 69.
[38] G. Xiong, V.S. Sullivan, P.C. Stair, G.W. Zajac, S.S. Trail, J.A. Kaduk, J.T. Golab, J.F. Brazdil, J. Catal. 230 (2005) 317.